Available online at www.sciencedirect.com

ScienceDirect

Geochimica et Cosmochimica Acta 166 (2015) 92–104

Geochimica et Cosmochimica Acta

www.elsevier.com/locate/gca

Fractionation of iron isotopes during leaching of natural particles by acidic and circumneutral leaches and development of an optimal leach for marine particulate iron isotopes

Brandi N. Revels [a], Ruifeng Zhang [b], Jess F. Adkins [c], Seth G. John [a,*]

[a] Department of Earth and Ocean Sciences, University of South Carolina, Columbia, SC 29208, United States
[b] State Key Laboratory of Estuarine and Coastal Research, East China Normal University, Shanghai, China
[c] Geological and Planetary Sciences, California Institute of Technology, Pasadena, CA, United States

Received 30 October 2014; accepted in revised form 19 May 2015; available online 30 May 2015

Abstract

Iron (Fe) is an essential nutrient for life on land and in the oceans. Iron stable isotope ratios (δ^{56}Fe) can be used to study the biogeochemical cycling of Fe between particulate and dissolved phases in terrestrial and marine environments. We have investigated the dissolution of Fe from natural particles both to understand the mechanisms of Fe dissolution, and to choose a leach appropriate for extracting labile Fe phases of marine particles. With a goal of finding leaches which would be appropriate for studying dissolved-particle interactions in an oxic water column, three particle types were chosen including oxic seafloor sediments (MESS-3), terrestrial dust (Arizona Test Dust – A2 Fine), and ocean sediment trap material from the Cariaco basin. Four leaches were tested, including three acidic leaches similar to leaches previously applied to marine particles and sediments (25% acetic acid, 0.01 N HCl, and 0.5 N HCl) and a pH 8 oxalate-EDTA leach meant to mimic the dissolution of particles by organic complexation, as occurs in natural seawater. Each leach was applied for three different times (10 min, 2 h, 24 h) at three different temperatures (25 °C, 60 °C, 90 °C). MESS-3 was also leached under various redox conditions (0.02 M hydroxylamine hydrochloride or 0.02 M hydrogen peroxide). For all three sample types tested, we find a consistent relationship between the amount of Fe leached and leachate δ^{56}Fe for all of the acidic leaches, and a different relationship between the amount of Fe leached and leachate δ^{56}Fe for the oxalate-EDTA leach, suggesting that Fe was released through proton-promoted dissolution for all acidic leaches and by ligand-promoted dissolution for the oxalate-EDTA leach. Fe isotope fractionations of up to 2‰ were observed during acidic leaching of MESS-3 and Cariaco sediment trap material, but not for Arizona Test Dust, suggesting that sample composition influences fractionation, perhaps because Fe isotopes are greatly fractionated during leaching of silicates and clays but only minimally fractionated during dissolution of Fe oxyhydroxides. Two different analytical models were developed to explain the relationship between amount of Fe leached and δ^{56}Fe, one of which assumes mixing between two Fe phases with different δ^{56}Fe and different dissolution rates, and the other of which assumes dissolution of a single phase with a kinetic isotope effect. We apply both models to fit results from the acidic leaches of MESS-3 and find that the fit for both models is very similar, suggesting that isotope data will never be sufficient to distinguish between these two processes for natural materials. Next, we utilize our data to choose an optimal leach for application to marine particles. The oxalate-EDTA leach is well-suited to this purpose because it does not greatly fractionate Fe isotopes

* Corresponding author.
E-mail address: sjohn@geol.sc.edu (S.G. John).

http://dx.doi.org/10.1016/j.gca.2015.05.034

for a diversity of particle types over a wide variety of leaching conditions, and because it approximates the conditions by which particulate Fe dissolves in the oceans. We recommend a 2 h leach at 90 °C with 0.1 M oxalate and 0.05 M EDTA at pH 8 to measure labile "ligand-leachable" particulate δ^{56}Fe on natural marine materials with a range of compositions.

1. INTRODUCTION

Iron is an essential micronutrient for all organisms. In terrestrial environments, iron in soils is an important micronutrient both for plants and soil microbes. Soil Fe deficiency can lead diseases such as chlorosis in plants (Epstein, 1971), and soil bacteria often produce siderophores both to aid their own acquisition of Fe and to sequester Fe away from competing species (Lovely, 2000). Despite the abundance of Fe in the earth's crust and on land, Fe is scarce in seawater. Fe is relatively insoluble in seawater compared to other elements, and is typically present at concentrations lower than 1 nM (Bruland and Lohan, 2003). The obligatory requirement of phytoplankton for Fe, combined with it's often low concentrations in the surface ocean, mean that Fe is the limiting nutrient for phytoplankton growth in large regions of the world ocean (Moore and Braucher, 2008; Moore et al., 2013). Iron stable isotope ratios (δ^{56}Fe) are an important tool to study the chemical and biological reactions of Fe, and they have previously been used to study the exchange of Fe between particles, such as soil or suspended marine particulate matter, and dissolved phases, in experimental, terrestrial, and marine environments.

Particulate forms of Fe may be an important source of this micronutrient to the ocean. Particulate Fe concentrations in many parts of the ocean are higher than dissolved Fe concentrations (Collier and Edmond, 1984; Sherrell and Boyle, 1992), and particulate Fe supply in the form of atmospheric dust deposition, sediment resuspension, and glacial inputs are thought to support a significant portion of global phytoplankton growth (Raiswell et al., 2006; Hawkings et al., 2014) (Jickells et al., 2005; Lam et al., 2006; Lam and Bishop, 2008; Moore and Braucher, 2008). Analysis of marine particulate δ^{56}Fe provides a valuable tool for understanding how Fe cycles between particulate and dissolved phases in the ocean. For example, Radic et al. (2011) digested marine particles with aqua regia and HF in order to constrain the source of these particles. Similarly, Escoube et al. (2009) and Gelting et al. (2010) have used total digests of particulate Fe in estuarine and coastal environments to determine particle provenance. Within anoxic ocean basins, where various Fe minerals precipitate and redissolve at redox interfaces, Staubwasser et al. (2013) have applied a total particle digestion to study Fe speciation and reaction, and in a separate study applied a dithionite-citrate leach to access the "reactive" Fe followed by total digestion (Staubwasser et al., 2006). Bennett et al. (2009) digested particles in a hydrothermal plume by refluxing for 72 h in concentrated HNO_3 in order to study Fe isotope cycling in plumes and constrain the δ^{56}Fe of hydrothermal dissolved Fe to the ocean. Severmann et al. (2004) leached hydrothermal plume particles for 1 h in 0.1 N HCl to determine the "HCl extractable" δ^{56}Fe, followed by digestion in HNO_3. Waeles et al. (2007) applied a pH 4.7 ammonium acetate leach to marine aerosols in order to access the "readily soluble" fraction and postulate the dissolved δ^{56}Fe for dust impacted seawater. A similar variety of leaches has been applied to marine sediments. For example, Severmann et al. (2006) measured both pyrite δ^{56}Fe and total sediment δ^{56}Fe during a sequential extraction of anoxic sediments in order to examine Fe redox cycling in modern environments. Fehr et al. (2008) applied a sequential leach of cold 0.5 N HCl for 1 h to release "labile" Fe, followed by 23 h in cold 1 N HCl to release "reactive" Fe, then by several hours in HF at 150 °C to dissolve silicates, and finally aqua regia to dissolve pyrites, for a study of Fe isotope cycling in past anoxic sedimentary environments. Roy et al. (2012) used a leach of 0.25 M hydroxylamine hydrochloride in 0.25 M HCl followed by 1.0 M hydroxylamine hydrochloride in 25% acetic acid to extract the "leachable Fe-oxides" from estuarine sediments in order to study the mobilization and reprecipitation of Fe within porewater redox gradients.

There is also extensive literature on the fractionation of Fe isotopes during dissolution of natural rocks and minerals from terrestrial environments. Brantley and co-workers showed that lighter isotopes were preferentially dissolved from a silicate soil by organic acids and naturally-produced siderophores with difference between the bulk δ^{56}Fe and solution δ^{56}Fe ($\Delta\delta^{56}Fe_{solution\text{-}bulk}$) as low as −1 permil (‰) (Brantley et al., 2001). A combination of easily-extractable soil Fe phases was found to be about $\Delta\delta^{56}Fe_{solution\text{-}bulk} = -0.3‰$ compared to bulk soils (Guelke et al., 2010). Oxalate/oxalic acid and hydrochloric acid have been used in various studies examining Fe isotope fractionation. For example, Chapman et al. (2009) found that both 0.5 M HCl (pH 0.34) and 5 mM oxalic acid (pH 2.18) preferentially released lighter isotopes of Fe during early stages of the dissolution of granite and basalt, with initial solution $\Delta\delta^{56}Fe_{solution\text{-}bulk}$ between −0.8‰ and −1.4‰. The phyllosilicate clays biotite and chlorite were leached with pH 4 HCl and pH 4–6.5 mM oxalic acid, with larger isotopic fractionations found for HCl (as low as −1.4‰) compared to oxalic acid (−0.5‰) (Kiczka et al., 2010a). The fractionation of Fe isotopes upon mineral dissolution has been invoked to explain why large differences of up to several permil have been observed between the δ^{56}Fe of plants and the δ^{56}Fe of the soil in which they grew (Guelke and Von Blanckenburg, 2007; Guelke et al., 2010; Kiczka et al., 2010b; Guelke-Stelling and von Blanckenburg, 2012).

While many of these previous studies measured δ^{56}Fe in sediments, or used leaches originally developed for

sediments, this work is more focussed on relevance to measuring δ^{56}Fe of marine particles suspended in the water column. To that end we have studied three different particle types, an oxic marine sediment of the sort which might be resuspended from the seafloor, continental mineral dust as a proxy for aerosol Fe, and marine sediment trap material which contains a range of different Fe-bearing phases. The leaching conditions studied here are also based on relevance to marine water column work, including a pH 2 acetic acid leach with reductant previously used to extract 'labile' Fe from marine particles (Berger et al., 2008), a 0.5 N HCl leach similar to that used to determine marine suspended particulate Fe (Bishop et al., 1985), and a pH 8 oxalate-EDTA leach meant to mimic the dissolution of Fe by organic chelators, the process expected to dominate in the ocean where most dissolved Fe is bound to organic ligands (Rue and Bruland, 1995; Rauschenberg and Twining, 2015). We have tested these leaches and others under a wide range of time and temperature conditions in order to better understand how leachate δ^{56}Fe varies based on leach conditions, and therefore to better understand the mechanisms of Fe release and Fe isotope fractionation. Thus, the aims of this manuscript are twofold: (1) by relating Fe isotope fractionation to leach composition we hope to gain a better understanding of the mechanism by which Fe isotopes are released from particles and (2) by discovering which leaches have the smallest effect on the δ^{56}Fe of leached Fe, we hope to suggest a leach which is appropriate for accessing biogeochemically active labile Fe phases from a wide variety of different marine particles.

2. METHODS

2.1. Sample description

MESS-3 is a marine sediment reference material certified for trace metal concentrations (National Research Council of Canada). MESS-3 was collected in the Beaufort Sea (70° N, 133.5° W), and was homogenized, freeze-dried, and passed through a No. 120 (125 μm) screen before distribution. MESS-3 was collected in a region where both the water column and sediment porewaters are oxic, and is composed primarily of weathered continental silicates, as well as illite and other clay minerals (Naidu et al., 1971). MESS-3 has a certified Fe concentration of 4.34% by weight. In order to prevent aerosolization of mineral particles and facilitate measurement of small quantities by pipette, MESS-3 was mixed with trace-metal clean artificial seawater before use.

Arizona Test Dust (AZTD; ISO 12103-1 A2 Fine, Batch 11740F, Powder Technologies Incorporated) is made from natural soils collected in the southwestern US and sifted to include particles only in the 1–100 μm range. The most common particles within AZTD have Fe:Al:Si ratios consistent with crystalline aluminosilicate clay minerals, though particles containing high-Fe iron oxyhydroxides and iron silicates are also present in abundance (Cwiertny et al., 2008; Chen et al., 2012). AZTD contains 1.98% Fe by weight (Chen et al., 2012), with the most Fe-rich particles primarily in the smallest size fraction of particles less than ~3 μm (Cwiertny et al., 2008). AZTD was also mixed with artificial seawater before use.

Samples from the Cariaco Basin (10.5° N, 64.7° W) were obtained from a sediment trap located at 275 m depth, within the oxic portion of the water column, as part of the cooperative Carbon Retention in a Colored Ocean (CARIACO) program on March 14, 1997 (Martinez et al., 2007). Samples were freeze-dried, powdered, and homogenized before analysis, and contained 48.23% biogenic material and 24.99% lithogenic material by weight, with an Fe concentration of 1.26% (Martinez et al., 2007). Samples were not processed with trace-metal cleanliness specifically in mind, however considering the high Fe concentrations in these samples contamination is unlikely to be significant.

2.2. Reagent preparation

Polyethylene and polypropylene labware was cleaned with 1% Citranox, then acid cleaned for 7 days in 10% HCl and rinsed with ultrapure H_2O (UPW) prior to use. PFA vials were precleaned with concentrated HNO_3 and cleaned with 0.1% HNO_3 between uses. HCl and HNO_3 were prepared in a subboiling still to Fe concentrations of <10 ppt, and diluted with UPW with a blank of <1 ppt.

2.2.1. Primary leach preparation

Four primary leaches were tested on all three particle types, including an HCl 'strong' and 'weak' leach, an 'acetic acid' leach, and an 'oxalate-EDTA' leach (Table 1). The strong leach was prepared by diluting HCl to 0.5 N, and the pH 2 weak leach was prepared by diluting HCl to 0.01 N. The pH 2 acetic acid leach was prepared with 25% purified acetic acid (Aristar Ultra, BDH) and 0.02 M hydroxylamine hydrochloride (Acros, 99%+, #266-798-2, Lot A0294569). The oxalate-EDTA leach was prepared with high-purity chemicals including 0.05 M EDTA (Fisher BioReagents, tetraacetic acid form, #BP118-500, Lot 095965A), 0.1 M oxalic acid (Alfa Aesar 99.5%, #423150050, Lot A0284360), and was adjusted to pH 8 with NaOH (EMD ACS grade, #SX0593–1, Lot UN1832) according to the methods described by Tovar-Sanchez et al. (2003) and subsequently modified by Tang and Morel (2006), except NaCl was not added in order to simplify purification for isotopic analysis, and because high ionic strength was not needed to prevent cell lysis. Also, while the original oxalate-EDTA leach was meant to be applied to living cells and was specifically meant not to leach biogenic metals within the cells, our application of this leach solution includes a heating step and is applied to previously-dried material, meaning it will be much more likely to access biogenic Fe.

Several batches of the EDTA-oxalate leach solution were cleaned of Fe to varying extents according to the published procedures (Tovar-Sanchez et al., 2003). Briefly, Fe was reduced using hydroxylamine hydrochloride, reacted with perchlorate and 1,10-phenanthroline to bind Fe(II), and the Fe(II) was extracted into dichloroether. MESS-3 and Cariaco particles were leached with an oxalate-EDTA solution containing 80.0 ± 2.1 ng g^{-1} Fe with a δ^{56}Fe of

Table 1
A description of the different leaches applied to marine particles. The primary leaches were applied to all three particle types, while the secondary leaches were applied only to MESS-3.

Leach description	Composition	Temperatures	Times	References
Primary leaches				
Strong HCl	0.5 N HCl	25 °C, 60 °C, 90 °C	10 m, 2 h, 24 h	*
Weak HCl	0.01 N HCl	25 °C, 60 °C, 90 °C	10 m, 2 h, 24 h	
Oxalate-EDTA	0.1 M oxalic acid, 0.05 M EDTA, pH 8 with NaOH	25 °C, 60 °C, 90 °C	10 m, 2 h, 24 h	
Acetic acid	25% acetic acid, 0.02 M hydroxylamine HCl	25 °C, 60 °C, 90 °C	10 m, 2 h, 24 h	**
Secondary leaches				
n/a	Various	10 m at 90 °C, 110 m at 25 °C		**

* A 0.5 N HCl, 60 °C, 24 h leach was used in Lam et al. (2006) and Lam and Bishop (2008).
** As described by Berger et al. (2008).

$-0.37 \pm 0.17‰$ (1σ SD, $n = 3$), and AZTD was leached with a solution containing 10 ± 0.1 ng g^{-1} Fe with a δ^{56}Fe of $-6.65 \pm 0.15‰$ (1σ SD, $n = 2$). Final sample Fe concentrations and δ^{56}Fe values were determined by subtracting this blank contribution.

2.2.2. Secondary leaches

A smaller number of tests were performed, on MESS-3 only, with seven additional leaches. This group of leaches was termed "secondary" leaches because they were only tested on MESS-3 and were not the primary focus of our experiments. These leaches were tested under the temperature conditions proposed by Berger et al. (2008) to access "labile" particulate phases of Fe, which involved 10 min of leaching at 90 °C followed by 110 min leaching at room temperature. Leaches tested under these temperature conditions included 5% HCl (0.6 N) with either 0.02 M hydroxylamine hydrochloride, 0.02 M hydrogen peroxide (Aristar Ultra, BDH), or no addition. Similarly, a 1 M pH 2 sulfuric acid leach was prepared with H_2SO_4 (Aristar Ultra, BDH) and NaOH, both plain and amended with hydroxylamine hydrochloride or hydrogen peroxide. The acetic acid leach described above was also tested under these temperature conditions.

2.3. Experimental conditions

Prior to leaching experiments, MESS-3 and AZTD were filtered onto an acid-cleaned polyethersulfone (Supor) 0.45 μm filters. Filters were folded gently and placed in a 15 mL vial (Metal-Free, VWR), and exposed to treatment at a sample/leach ratio no higher than 1 mg/mL. Dry Cariaco sediment trap samples were added directly to vials for weighing and reaction at a sample/leach ratio no higher than 2 mg/mL. Particle samples were then amended with leach solution and reacted at room temperature (25 °C) or in a laboratory oven (60 °C and 90 °C), and at various times including 10 m, 2 h, and 24 h. After reaction, leachate was transferred to an HDPE/PP syringe (AirTite, Norm-Ject) and filtered through an acid-cleaned polypropylene 0.45 μm syringe filter (Whatman). The reaction vial was then rinsed with 1 mL UPW, and this was put through the syringe filter to expel any remaining leachate.

Total digests of all particle samples were prepared by reacting 10 mg of sample with 750 μL HF and 250 μL HNO_3 in a PFA vial on a hot plate at approximately 150 °C for 48 h to dissolve silicates. The samples were then evaporated, and twice reconstituted in 200 μL concentrated HCl and reevaporated in order to drive off residual fluoride before further purification.

2.4. Iron concentration and isotopic analysis

Initial iron concentration in the leachate were determined by reduction and reaction with ferrozine (Viollier et al., 2000) for all samples except the oxalate-EDTA leach. Because oxalate and EDTA compete with ferrozine to bind Fe(II), these samples were analyzed for initial Fe concentrations in medium resolution mode on a Thermo Element ICPMS after dilution to 1% in 0.1 N HNO_3. The final reported Fe concentrations in the leachate were determined after isotopic analysis by double-spike ICPMS, using isotope dilution. Because some of the leachate and rinse was typically retained in the reaction vessel and syringe filter, concentration accuracy depends on estimation of the final sample volume, subject to estimated errors of 5%.

After analysis of initial Fe concentrations, leachate containing 100 ng of Fe from each sample was amended with 200 ng of an Fe double-spike consisting of approximately equal concentrations ^{57}Fe and ^{58}Fe, using spike and sample ratios optimized to minimize analytical error (John, 2012). Samples were then dried down in clean PFA vials and reacted overnight with 100 μL each of concentrated HNO_3 and H_2O_2 to oxidize residual organics. Samples were then reconstituted in 200 μL 10 N HCl + 0.001 M H_2O_2 and purified by anion exchange chromatography using a method adapted for slightly smaller resin volume from previously published techniques (Borrok et al., 2007). Samples were loaded onto 120 μL of AG-MP1 anion exchange resin, salts were eluted with 0.5 mL 10 N HCl + 0.001 M H_2O_2, Cu was eluted with 1.2 mL 5 N HCl + 0.001 M H_2O_2, and Fe was eluted with 0.8 mL 2 N HCl. This eluent was then dried down and samples were reconstituted in 2 mL 0.1 N HNO_3 for isotopic analysis.

Fe stable isotopes were analyzed on a Thermo Neptune multi-collector ICPMS in high-resolution mode, according to analytical procedures developed for the analysis of Fe stable isotopes in seawater (Conway et al., 2013). Briefly, samples were introduced at a concentration of 50 ppb sample and 100 ppb double-spike using an Apex-Q (ESI)

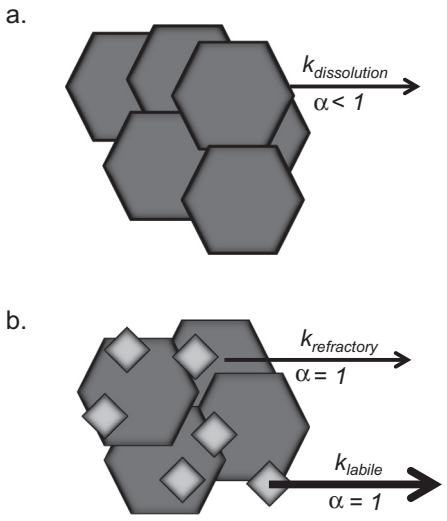

Fig. 1. Our conceptual model of two possible reasons for the observed variation in dissolved δ^{56}Fe as the fraction of Fe dissolved increases for acidic leaches. A kinetic isotope effect model assumes only one mineral phase, which is subject to a kinetic isotope effect during dissolution such that lighter isotopes are preferentially dissolved first (a). A two-phase mixing model assumes that there are two separate Fe-containing phases with different δ^{56}Fe, which dissolve at different rates (b).

desolvating introduction system, without a desolvating membrane, and measured for approximately 3 min. Isobaric interferences from Cr and Ni were corrected for by monitoring ^{53}Cr and ^{60}Ni, respectively, and instrumental mass bias was corrected for using the double-spike. Process blanks for the entire method were <5 ng, and analytical errors were typically about 0.03‰.

2.5. Fe isotope modeling

Two different models were developed to explore the relationship between the fraction of Fe leached from particles (F) and the isotopic composition of the leach (δ^{56}Fe) (Fig. 1). Our first model assumes a single uniform Fe phase, but allows for a fractionation by a kinetic isotope effect during dissolution, referred to here as a "KIE model." Our second model assumes two different phases, with two different δ^{56}Fe, which dissolve at different rates, referred to here as a "two-phase mixing model". Both models were fit to data from the acidic leaches of MESS-3. Both models were tested as all of the free parameters were varied, in order to determine the conditions under which R^2 was minimized.

2.5.1. KIE model

For the KIE model, we first assume that particles contain an outer layer which is in contact with the leach solution and available for dissolution, and an interior which does not dissolve until it is exposed to the leach solution when other Fe atoms are removed from the surface. It is therefore necessary to distinguish the pool of Fe atoms which are on the surface of the particle before leaching (pool 'SURF') from the pool of Fe atoms in the particle interior (pool 'INT'). At all times, Fe atoms removed from the surface will have an isotopic composition equal to the surface δ^{56}Fe plus the kinetic isotope effect for leaching. At first, the surface δ^{56}Fe will match total particle δ^{56}Fe, and thus the isotopic composition of Fe leached from the particle surface will be given by:

$$\delta^{56}Fe_{total-KIE} = \delta^{56}Fe_{total} - \Delta\delta^{56}Fe_{KIE} \quad (1)$$

where $\delta^{56}Fe_{total\text{-}KIE}$ is the isotopic composition of leached Fe which began as Fe on the surface, $\delta^{56}Fe_{total}$ is the total particle δ^{56}Fe, and $\Delta\delta^{56}Fe_{KIE}$ is the isotope effect for leaching. As the surface is leached, an equal area of the interior becomes exposed, and isotope mass balance dictates that the δ^{56}Fe of this newly exposed Fe will be equal to total δ^{56}Fe minus the isotope effect for leaching. Thus, this newly exposed Fe will have an isotope composition of $\delta^{56}Fe_{total} + \Delta\delta^{56}Fe_{KIE}$, and dissolved Fe released from INT pool will have an isotopic composition of $\delta^{56}Fe_{total}$.

The relative amounts of Fe dissolved from the surface ($SURF_{diss}$) and the interior (INT_{diss}) of the particle are next determined as a function of the proportion of total particulate Fe which is dissolved. The outer layer is assumed to dissolve by first-order kinetics by:

$$SURF_{diss} = SURF_o - SURF_o e^{-r} \quad (2)$$

where $SURF_o$ is the amount of Fe in the surface layer before exposure to the leach, and r is the e-folding time of the reaction under the specific leach conditions. By converting the typical reaction rate constant and time (e.g. $k{\cdot}t$) to a dimensionless parameter reflecting the extent of reaction (r), we can directly compare results from various acidic leaches, even though leaching occurred more quickly at higher temperatures and with stronger acids. We assume that the same mechanism is involved in particle dissolution regardless of the temperature and/or acid strength, and that all leaches therefore proceed in the same way with respect to r. As the original surface layer is depleted by dissolution, it is replaced by an equal quantity of Fe from the interior so that the total rate of Fe dissolution doesn't change. The total amount of Fe which has dissolved from both the surface and the interior of the particle can therefore be described by:

$$SURF_{diss} + INT_{diss} = SURF_o \cdot r \quad (3)$$

The fraction of total particle Fe which has been dissolved is:

$$F = \frac{SURF_{diss} + INT_{diss}}{SURF_o + INT_o}. \quad (4)$$

and the quantity of Fe on the particle interior can be related to the amount of Fe on the surface as:

$$J = INT_o/SURF_o \quad (5)$$

Eqs. (2–5) can then be combined to calculate the fraction of dissolved Fe from the surface (f_{SURF}) and from the particle interior (f_{INT}) as a function of F and J, which can be substituted into the isotope mass balance equation:

$$\delta^{56}Fe_{diss} = \delta^{56}Fe_{SURF} \cdot f_{SURF} + \delta^{56}Fe_{INT} \cdot f_{INT} \quad (6)$$

to yield:

$$\delta^{56}Fe_{diss} = \frac{\delta^{56}Fe_{total-KIE}(1-e^{(-F-FJ)}) + \delta^{56}Fe_{total}(F-FJ-1-e^{(-F-FJ)})}{(F+FJ)} \quad (7)$$

where $\delta^{56}Fe_{diss}$ is the total leachate isotope composition.

2.5.2. Two-phase mixing

For the two-phase mixing model, we assume that there are two phases which are exposed to the leach and which both dissolve according to first-order kinetics. We assume that one phase is more labile than the other, but that there is no isotopic fractionation of either phase during leaching (i.e. no kinetic isotope effect). The relative initial quantities of the refractory and labile phases are given by:

$$J = REF_0/LAB_0 \quad (8)$$

and their relative dissolution rate constants are given by:

$$j = r_{REF}/r_{LAB} \quad (9)$$

where REF_0 and LAB_0 are the initial quantities of refractory and labile Fe, and r_{REF} and r_{LAB} are the rate constants for dissolution of the refractory and labile phases, respectively. Assuming that both phases dissolve by first-order kinetics (as in Eq. (3)), the fraction of total Fe which has dissolved (F) is given by:

$$F = \frac{(1-e^{-r}+J-J\cdot e^{-jr})}{(1+J)} \quad (10)$$

Separately, we can solve for the total leachate $\delta^{56}Fe$ ($\delta^{56}Fe_{diss}$) as a function of r, by combining the isotope mass balance equation (as in Eq. (6)) with the equations for first-order dissolution of both phases to yield:

$$\delta^{56}Fe_{diss} = \frac{\delta^{56}Fe_{LAB}(1-e^{-r}) + \delta^{56}Fe_{REF}\cdot J(1-e^{(-rj)})}{(1-e^{-r}+J-Je^{(-rj)})} \quad (11)$$

where $\delta^{56}Fe_{LAB}$ and $\delta^{56}Fe_{REF}$ are the iron isotope compositions of the labile and refractory phases, respectively. While it is possible to combine Eqs. (9) and (10) to solve for $\delta^{56}Fe_{diss}$ as a function of F, the solution includes complex numbers and is therefore not simple to work with. Instead, we establish the relationship between $\delta^{56}Fe_{diss}$ and F by solving for both over a wide range of r.

3. RESULTS

3.1. Oxalate-EDTA leach cleaning

Cleaning the oxalate-EDTA solution lowered both the Fe concentration and the $\delta^{56}Fe$ (Fig. 2). Seven successive rounds of cleaning lowered the leach [Fe] from 288 ppb to 10 ppb, and lowered $\delta^{56}Fe$ from +0.26‰ to −6.65‰. Two leaches with intermediate amounts of cleaning contained 80 and 25 ppb of Fe, with $\delta^{56}Fe$ of −0.37‰ and −3.62‰, respectively. Thus, both [Fe] and $\delta^{56}Fe$ decreased together. The best fit for the data with a Rayleigh distillation model was obtained with a 1.82‰ isotope effect. The fact that isotopically heavy Fe was preferentially removed from solution suggests that this was not due to a redox equilibrium isotope effect, because Fe(II) is the species which is complexed by 1,10-phenanthroline and removed,

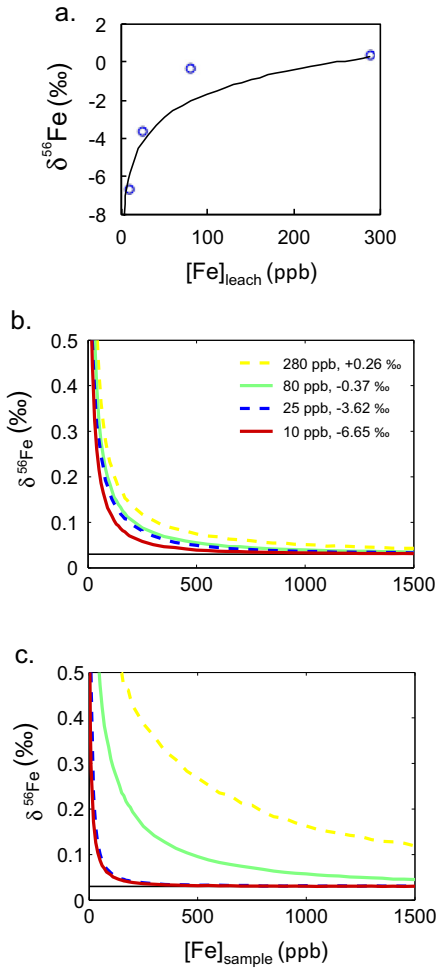

Fig. 2. Error in sample $\delta^{56}Fe$ over a range of sample concentrations for four different EDTA-oxalate leach solutions (a). Error is shown assuming a sample $\delta^{56}Fe$ of +1‰ (b) and −3‰ (c), which spans the range observed for most natural Fe samples. Lines represent the four solutions tested, with lower [Fe] after cleaning generally corresponding to lower $\delta^{56}Fe$. The horizontal grey line represents as assumed sample analytical error of 0.03‰.

and Fe(II) is typically about 3‰ lighter than Fe(III) at equilibrium (Johnson et al., 2002). Instead, perhaps the heavier Fe(II) isotopes are preferentially bound to 1,10-phenanthroline, consistent with theoretical predictions that heavier isotopes are concentrated in stronger binding environments such as organic ligands (Dideriksen et al., 2008).

3.2. Natural particle leaching

3.2.1. Primary leach results

The combination of 4 primary leaches, 3 leach times, and 3 leach temperatures resulted in 36 separate sets of leaching conditions, which were tested on 3 different particle types for a total of 108 different experimental conditions. Each experimental condition was tested in duplicate for a total of 216 possible samples, though 8 were lost due to sporadic sample mishandling leaving 208 samples

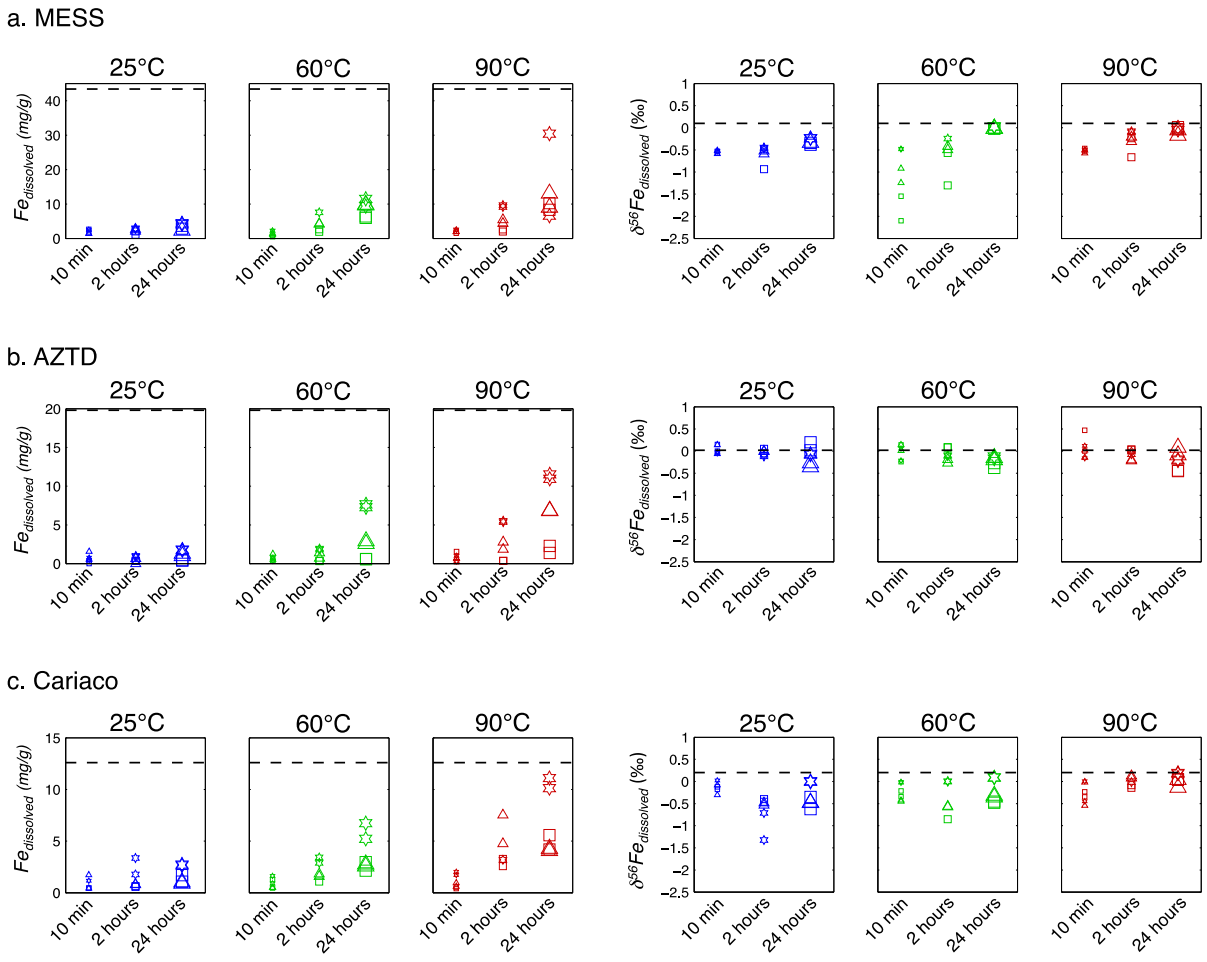

Fig. 3. Iron concentrations and stable isotope ratios for three different acidic leaches tested on materials including the MESS-3 sediment standard (a), Arizona Test Dust (b), and Cariaco basin sediment trap samples (c). Leaches included 0.5 M HCl (stars), 0.01 M HCl (squares) and 25% acetic acid +0.02 M hydroxylamine hydrochloride (triangles). Leaches were applied for 10 min, 2 h, and 24 h, at 25 °C, 60 °C and 90 °C. Dashed lines represent total particulate [Fe] and δ^{56}Fe.

for which we analyzed the concentration of Fe and δ^{56}Fe of the leachate (Table S1).

For all leaches tested, we observed a trend of increasing dissolution of Fe from particles with longer leaching times and at higher temperatures (Fig. 3). The strong leach consistently released the most Fe, but there was not a consistent pattern among the other three leaches tested (weak, acetic, and oxalate-EDTA) when comparing results for the same time and temperature. The total fraction of particle Fe leached ranged from 0.3 to 70% for MESS, 0.9 to 78% for AZTD, and 3 to 88% for Cariaco sediment trap material. Of the 108 experiments performed, 100 were performed in duplicate and the average difference between these duplicates was 4% for MESS, 2% for AZTD, and 6% for Cariaco sediment trap material. The error for duplicates was thus much less than the overall variability in Fe concentration for different leaches, highlighting the importance of time and temperature as controls on Fe dissolution rate.

There was also usually a correlation between longer leaching times and higher temperatures and higher δ^{56}Fe. However, this correlation did not hold true in all cases. A positive correlation between leaching time/temp and δ^{56}Fe was observed most strongly for acidic leaches of MESS-3 and Cariaco sediment trap material. There was not a clear relationship between leaching time/temp and δ^{56}Fe for the oxalate-EDTA leach applied to any sample types. For AZTD, there was a slight negative correlation between leach time/temp and δ^{56}Fe.

Because time, temperature, and leach type all simultaneously affected the amount of Fe leached from the particles and the δ^{56}Fe of the leachate, we examine the leachate δ^{56}Fe as a function of the fraction of Fe leached from the particles (F) (Fig. 4). Doing so revealed that the relationship between F and δ^{56}Fe was different depending on particle type and on whether the leach was acidic (strong, weak, and acetic) or circumneutral (oxalate-EDTA). For each particle type, a consistent relationship between F and δ^{56}Fe was found for all of the acidic leaches, and a separate relationship was observed for the oxalate-EDTA leach.

3.2.2. Secondary leach results

Each of the 7 secondary leaches were tested in duplicate or triplicate on MESS-3, resulting in 18 additional samples (Table S1). The leaches prepared with 0.6 N HCl

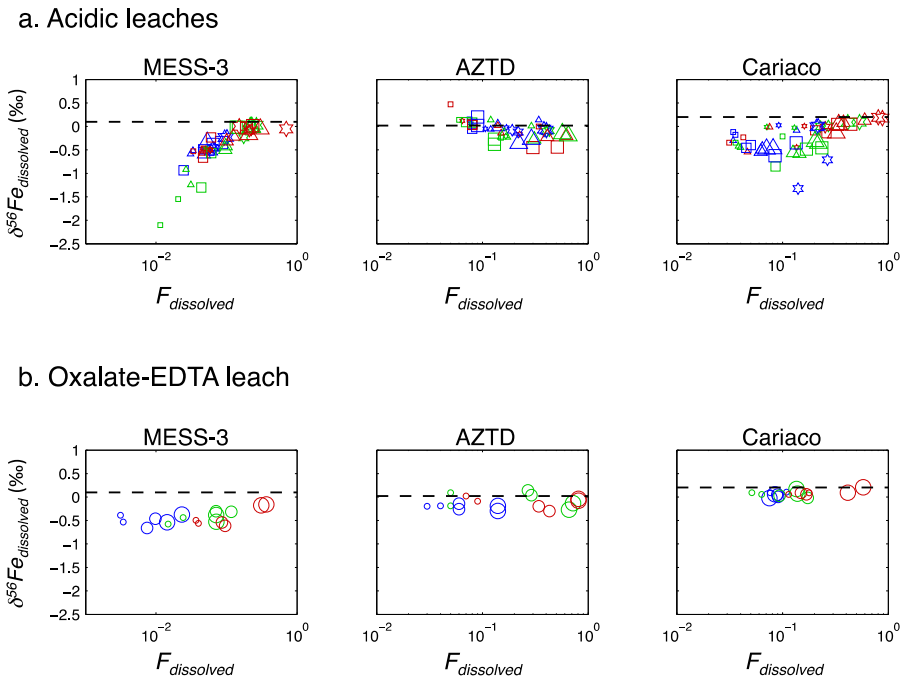

Fig. 4. Dissolved iron stable isotope ratios (δ^{56}Fe) compared to the fraction of total particulate Fe which has been dissolved ($F_{dissolved}$). Data is shown separately for the acidic leaches (a) and the EDTA-oxalate leach (b). Symbol size corresponds to leaching time with small, medium, and large symbols representing 10 min, 2 h, and 24 h leaches, respectively. Symbol color corresponds to temperature with blue, green, and red corresponding to 25 °C, 60 °C and 90 °C, respectively. Symbol shape corresponds to leach type with stars, squares, triangles, and circles corresponding to 0.5 M HCl, 0.01 M HCl, 25% acetic acid +0.02 M hydroxylamine hydrochloride, and EDTA-oxalate, respectively. The black dashed horizontal line corresponds to total particle δ^{56}Fe. Data from the 90 °C leaches of Cariaco material with oxalate-EDTA (4b, red circles, right-hand figure) also appears in Revels et al. (2014). (For interpretation of the references to colour in this figure legend, the reader is referred to the web version of this article.)

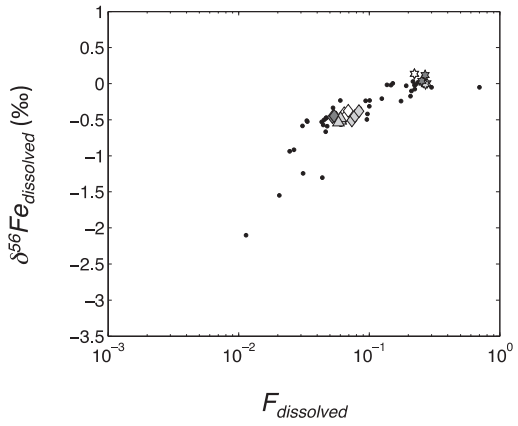

Fig. 5. Iron stable isotope ratios compared to the fraction of Fe dissolved from MESS-3 particles by the secondary leaches described in Section 2.2.2. Results are shown for 0.6 N HCl (stars), pH 2 sulfuric acid (diamonds), and pH 2 acetic acid (triangles), either with no added reductant or oxidant (white), with 0.02 M hydroxylamine hydrochloride reductant (light grey), or 0.02 M hydrogen peroxide oxidant (dark grey). Results from the primary leaches of MESS-3 are pictured for comparison (black circles).

consistently leached higher quantities of Fe compared to the pH 2 sulfuric acid and acetic acid leaches, similar to the primary leaches tested. The final δ^{56}Fe in 0.6 N HCl leaches was also higher than for the pH 2 leaches, which was also similar to results from the primary leaches. When comparing leachate δ^{56}Fe to F, results from the secondary leaches were similar to results from the primary leaches (Fig. 5). Neither the type of the acid used for the pH 2 leaches (acetic acid versus sulfuric acid), nor the presence of a reductant and/or oxidant had a large impact on the leached δ^{56}Fe. However, for the sulfuric acid leach there was a slight increase in the fraction of Fe leached in the presence of a reductant, and a slight decrease in the presence of an oxidant.

4. DISCUSSION

4.1. Optimal cleaning for the oxalate-EDTA leach

Cleaning the oxalate-EDTA solution involves a tradeoff between lower levels of Fe contamination and an increasingly un-natural δ^{56}Fe. Assuming that most natural samples have a δ^{56}Fe close to 0‰, contamination with very fractionated δ^{56}Fe may influence sample δ^{56}Fe. The relative benefits of a cleaner, but more fractionated, leach were simulated by assuming a 5% measurement error in the final sample concentration. Over a range of sample δ^{56}Fe from −3‰ to +1‰, roughly equivalent to the total range measured for natural samples, we found that error was always minimized by using a leach with lower [Fe] (10 ppb), even though the leach δ^{56}Fe was significantly fractionated from natural (−6.65‰). Thus, we suggest extensive cleaning of

the oxalate-EDTA leach prior to using it on natural samples.

Error due to contamination in the leach solution can also be minimized by accurately determining the leach δ^{56}Fe and the fraction of total leachate Fe attributable to background blank. It is therefore advisable to determine leach background [Fe] and δ^{56}Fe as accurately as possible, and to know accurately how much leach was used, so that a good blank correction can be done to determine sample δ^{56}Fe.

4.2. Mechanisms of Fe isotope fractionation

For all three sample types, we observed a similar relationship between the fraction of Fe leached (F) and the leached δ^{56}Fe for all of the acidic leaches, and a different relationship between F and δ^{56}Fe for the oxalate-EDTA leach (Fig. 4). This suggests a similar chemical mechanism of proton-promoted Fe dissolution for all acidic leaches, and a similar ligand-promoted dissolution mechanism for all oxalate-EDTA leaches.

4.2.1. Acidic leaches

While the underlying mechanism of dissolution is inferred to be the same for all acidic leaches, each sample type exhibited a different relationship between F and the δ^{56}Fe of the leached Fe. For both MESS-3 and the Cariaco sediment trap samples, the acidic leaches preferentially removed isotopically light Fe early in the dissolution process. For the AZTD sample, there was not a preferential release of isotopically light Fe during early stages of leaching. Instead, there was a slight trend of heavier δ^{56}Fe released early in the dissolution process.

Fe isotope fractionation during dissolution by acidic leaches can therefore be tentatively attributed to the mixture of minerals present. Our sample with the highest proportion of Fe in silicates and phyllosilicates (MESS-3) exhibited a preferential release of lighter Fe early in the dissolution process, similar to the previous results from silicates (Chapman et al., 2009) and phyllosilicates (Kiczka et al., 2010a). Our sample with the highest amount of Fe as oxyhydroxides (AZTD) did not exhibit preferential early release of isotopically light Fe, similar to the experimental results on goethite dissolution (Wiederhold et al., 2006). For the Cariaco sediment trap sample, the intermediate amount of Fe isotope fractionation observed and the greater variability in δ^{56}Fe as a function of F could be attributed to a greater diversity and heterogeneity of Fe-containing phases within these samples.

The fact that MESS-3 dissolution rates were not very affected by leach redox conditions supports our hypothesis that dissolution was primarily proton-promoted. However, it should be noted that MESS-3 contained relatively little of the Fe oxyhydroxide species which are most sensitive to the addition of a reductant (Chester and Hughes, 1967; e.g. Berger et al., 2008). The impact of Fe reduction on Fe dissolution rates and Fe isotope fractionation for Fe oxyhydroxide-rich samples has therefore yet to be fully investigated.

4.2.2. Non-acidic leaches

For all three sample types, there was not as much Fe isotope fractionation during leaching with an oxalate-EDTA leach as compared to the acidic leaches. The average δ^{56}Fe of Fe dissolved from Cariaco sediment trap samples matched bulk sample δ^{56}Fe. While the δ^{56}Fe of Fe dissolved from MESS-3 and AZTD was 0.5‰ and 0.2‰ lighter than the bulk samples, respectively, this fractionation was still less than observed with acidic leaches.

Our finding that dissolution by the oxalate-EDTA leach did not greatly fractionate Fe isotopes is consistent with the work of Waeles et al. (2007), who found that a pH 4.7 ammonium acetate buffer did not significantly fractionate leached δ^{56}Fe compared to bulk African dust. However, our results are in contrast to the findings of Wiederhold et al. (2006) who found that ligand-promoted dissolution of goethite by oxalate fractionated Fe isotopes by up to 2‰ at pH 3. The difference between their findings and ours could be due to either to the particles used or to the leach used. Neither MESS-3 nor Cariaco sediment trap samples would be expected to contain large quantities of Fe oxyhydroxides. Mossbauer spectroscopy demonstrates the presence of abundant Fe oxyhydroxides in AZTD, but cannot distinguish whether this is hematite, goethite or other oxyhydroxide phases (Cwiertny et al., 2008). Alternatively, because the second pKa of oxalic acid is 4.3, the leach used by Wiederhold et al. would have contained primarily mono-protonated oxalate, while our solution would have contained mostly deprotonated oxalate, possibly affecting the mechanism of Fe dissolution.

4.2.3. Model comparison with data

Previous studies have ascribed the fractionation of Fe isotopes during leaching to one of two very different processes, either a two-phase model of particle dissolution or to kinetic isotope effects (KIEs) during dissolution. Early release of lighter Fe during dissolution of granite and basalt was attributed to the presence of an isotopically light pool of Fe which dissolved more rapidly than the bulk mineral (Chapman et al., 2009) as was preferential release of lighter Fe from soils, compared to a total digest (Wiederhold et al., 2007). Early release of lighter Fe isotopes during oxalate dissolution of goethite and during acidic dissolution of phyllosilicates was attributed to a kinetic isotope effect (Kiczka et al., 2010a). Our new analyses of δ^{56}Fe during the acidic dissolution of MESS-3 provide the largest dataset to date on the relationship between F and δ^{56}Fe, providing a good opportunity to test both models.

The "two-pool" and "KIE" models used here are mathematically similar to models presented previously in the literature. Our two-phase model is similar to a model developed by Chapman et al. (2009), which assumed a labile pool of Fe which dissolves instantaneously, and a refractory pool of Fe which subsequently mixes with labile Fe. However, our model represents a slightly more realistic case in which both labile and refractory Fe dissolve simultaneously, while the model of Chapman et al. assumed complete dissolution of the labile phase before any of the refractory phase dissolved. Our KIE model is similar to

that of Wiederhold et al. (2006). The main advantage of the model formulation here is that we provide an analytical solution, where Wiederhold presented a numerical solution. The analytical solution is less computationally intensive and is likely to be simpler to implement for those without programming experience. The most important advantage of the approach taken here, however, is not that our models represent a substantial theoretical improvement over earlier models. Rather, it is that we present both models together in a similar framework so that their output can be easily compared.

Comparing our two models demonstrates that the two-pool model and the KIE model can produce very similar results (Fig. 6), and thus that Fe concentrations and δ^{56}Fe alone are not sufficient to distinguish between these processes. For the range of F values over which the models were fit to data, the best-fit curves for the two models never differed by more than 0.1‰. Thus, even in an experimental system where the particle mineralogy is well known, it would be necessary to have some additional constraints on the model equations, such as a priori knowledge of J or j, in order to use Fe isotopes to determine whether observed isotopic fractionation is due to the presence of two different phases with different δ^{56}Fe, or a kinetic isotope effect during fractionation.

Of course, for natural particles both of these models probably represent an oversimplification. Fe isotope fractionation systematics will be even less well constrained for natural particles where there may be multiple phases present and every phase may have a different kinetic isotope effect. For example, we find greater variability in the relationship between F and δ^{56}Fe for the Cariaco sediment trap samples, which contain a wide variety of different Fe phases, than for MESS-3. This modeling exercise therefore highlights the near impossibility of determining what controls Fe isotope fractionation in natural systems, and demonstrates that just because a two-phase model or a KIE model provides a reasonable fit to the data should not be taken as an indication that the model is correct.

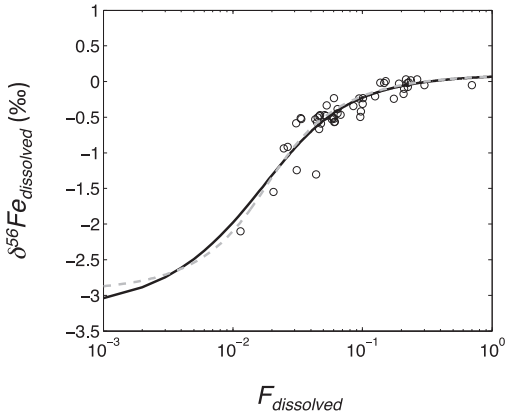

Fig. 6. Best-fit model output for a kinetic isotope effect model (black solid line) and a two-phase model (dashed grey line) to the data for all acidic leaches of the MESS-3 sediment material.

4.3. An optimal leach for marine particulate δ^{56}Fe

Results of δ^{56}Fe release during particle dissolution can be applied to choose an optimal leach for marine natural particles. Finding an appropriate leach for marine particulate Fe is challenging because of the tremendous diversity in particulate Fe in different marine environments. Especially within the context of GEOTRACES, a program which aims to measure dissolved and particulate trace metals throughout the world ocean, marine particles may come from a wide variety of environments. Some previous oceanographic studies have pursued a total digestion of marine particles for δ^{56}Fe, in which case there is no need to worry about isotopic fractionation during leaching (Severmann et al., 2004; Bennett et al., 2009; Escoube et al., 2009; Gelting et al., 2010; Radic et al., 2011; Staubwasser et al., 2013). However, in many marine settings, the total particulate Fe pool is dominated by silicates and other refractory phases which are non-biogeochemically active. In this case, it would be valuable to have a leach which can access "biogeochemically active Fe" phases. These would include biological phases such as biogenic tissue and detritus, hydrogenic minerals which precipitated directly from seawater such as Fe oxyhydroxides, and authigenic minerals precipitated from sediment porewaters such as Fe oxyhydroxides and Fe sulfides.

Most previously-published leaches for marine particulates which aim to extract labile δ^{56}Fe are acidic (Severmann et al., 2006; e.g. Fehr et al., 2008; Roy et al., 2012; Staubwasser et al., 2013). However, our results suggest that acidic leaches are a poor choice for many types of marine particles when the goal is to analyze Fe isotopes, especially for weaker leaches which dissolve less than ~10% of total Fe. We find that leach δ^{56}Fe for acidic leaches is highly dependent on the amount of Fe leached for MESS-3 and Cariaco sediment trap samples. Thus, the δ^{56}Fe of the leach will be highly dependent on the specific conditions used to leach the samples. Changes in temperature and/or leach time could have a large impact on the reported leachate δ^{56}Fe, meaning that δ^{56}Fe will not be a reliable reporter for particle biogeochemistry. Of course, our findings that acidic leaches are a poor choice for many types of marine samples does not necessarily mean that previous work is invalid. Indeed, most previous applications of leaches for δ^{56}Fe have been in sediments or water column environments with high concentrations of Fe oxyhydroxides. These samples may be very different from MESS-3 and Cariaco sediment trap samples which contain high proportions of silicates, clays, and biogenic material. For AZTD, our sample with the largest proportion of Fe as oxyhydroxides, acidic leaches did not greatly fractionate Fe isotopes.

In contrast to the acidic leaches, our data suggest that a pH 8 oxalate-EDTA leach is a good choice for leaching marine particle samples which include a complex mixture of many different materials for δ^{56}Fe. Of course, it is impossible to know whether a certain leach will fractionate Fe isotopes during dissolution of a new particle type without testing. However, the relatively small variability in δ^{56}Fe as a function of F for the three very different types of

marine particles tested here suggests that the oxalate-EDTA leach is likely to be relatively insensitive to leaching conditions for many different particle types. For our work, we have decided to use a leach of 2 h at 90 °C, which is at a high enough temperature to denature organic material and over a long enough time to be simple to execute. Importantly, our results suggest that the δ^{56}Fe in the leachate is relatively similar for the oxalate-EDTA for a large range of values of *F*, and thus an important characteristic of this leach is that δ^{56}Fe is relatively insensitive to the leaching conditions used.

The oxalate-EDTA leach also approximates the conditions under which particulate Fe could dissolve in the real ocean. Under oxic conditions, more that 99% of Fe in seawater is bound to organic ligands (Rue and Bruland, 1995; Wu and Luther, 1995). While the structure of these ligands is unknown, they are known to have hydroxamate and catecholate binding groups similar to those present in EDTA and oxalic acid (Barbeau, 2006). Though our leach contains much higher ligand concentrations and occurs at higher temperatures, the underlying chemical mechanism of dissolution is likely to be similar as for natural seawater.

While we believe that the oxalate-EDTA leach is well suited to δ^{56}Fe studies on natural marine particles of the sort examined here, it may not be appropriate for other applications. The oxalate-EDTA leach is not expected to dissolve silicates, and thus it is expected to be more representative of the "biogeochemically active Fe" pool than a total digestion, but the exact nature of the phases which are accessed by this leach has not been studied in depth. Therefore, in studies which seek to quantify the amount of Fe in a particular phase, it may be preferable to use leaches explicitly designed to access that specific phase. For suspended particles in seawater, a wide variety of techniques have recently been compared in order to find determine the optimum approach for measuring "biogenic" Fe (Rauschenberg and Twining, 2015), and several leaches were compared for their ability to access "labile Fe" (Berger et al., 2008). For sediments, there is a long history in the literature of studies which aim to sequentially leach specific Fe-bearing phases (e.g. Tessier et al., 1979; Poulton and Canfield, 2005). Finally, we have focussed here only on particles from oxic environments, and so we do not know how Fe quantities or δ^{56}Fe would behave in leaches of particles from reducing environments where Fe(II) minerals and sulfides are present.

5. CONCLUSIONS

The dataset presented here is one of the largest exploring Fe isotope fractionation during leaching of natural particles. For all three sample types tested, we find that there is a similar relationship between the amount of Fe leached and δ^{56}Fe for all of the acidic leaches. For the pH 8 oxalate-EDTA leach, we find for all three sample types that the relationship between the amount of Fe leached and δ^{56}Fe is very different from the acidic leaches.

The large amounts of isotopic fractionation observed during acidic leaching of MESS-3 and Cariaco sediment trap samples can be explained either by the mixing between Fe from two different phases with different δ^{56}Fe, or by a kinetic isotope effect during dissolution. We present the first analytical solutions for both a two-phase mixing model and a kinetic isotope effect model, and show that their fits to the data can be very similar. By comparing our model output with data from acidic leaches of MESS-3, we conclude that [Fe] and δ^{56}Fe alone are not sufficient to distinguish between these models.

Finally, we propose a new leach for measuring "biogeochemically active Fe" in natural marine particles. Our results show that the δ^{56}Fe of Fe leached from particles does not change very much as more Fe is dissolved when using a pH 8 oxalate-EDTA leach. This leach is therefore a good candidate for accessing labile Fe from natural particles that may contain a wide variety of different Fe-containing phases, without concern that δ^{56}Fe will be highly dependent on leach conditions. We recommend a 2 h application of this leach at 90 °C because the high temperature will facilitate release of biogenic Fe, and the time is long enough for simple application, but short enough to limit high Fe release to the more labile phases. Application of this leach for natural samples may help us to better understand the role of particles in the marine biogeochemical cycling of Fe, particularly for projects such as the GEOTRACES initiative, where large-scale sampling means that particles with a wide variety of compositions will be collected.

ACKNOWLEDGEMENTS

The authors would like to thank Angela Rosenberg and Beth Bair for technical assistance with isotopic analyses, and Bob Thunell for providing Cariaco sediment trap samples. This work was supported by National Science Foundation Grants OCE-1131387 and OCE-1334029. RZ was supported by The National Natural Science Foundation of China Grant 41006043. This manuscript was significantly improved by the suggestions of three anonymous reviewers.

APPENDIX A. SUPPLEMENTARY DATA

Supplementary data associated with this article can be found, in the online version, at http://dx.doi.org/10.1016/j.gca.2015.05.034.

REFERENCES

Barbeau K. (2006) Photochemistry of organic iron(III) complexing ligands in oceanic systems. *Photochem. Photobiol.* **82**, 1505–1516.

Bennett S. A., Rouxel O., Schmidt K., Garbe-Schönberg D., Statham P. J. and German C. R. (2009) Iron isotope fractionation in a buoyant hydrothermal plume, 5°S Mid-Atlantic Ridge. *Geochim. Cosmochim. Acta* **73**, 5619–5634.

Berger C. J. M., Lippiatt S. M., Lawrence M. G. and Bruland K. W. (2008) Application of a chemical leach technique for estimating labile particulate aluminum, iron, and manganese in the Columbia River plume and coastal waters off Oregon and Washington. *J. Geophys. Res.* **113**, 16.

Bishop J. K. B., Schupack D., Sherrell R. M. and Conte M. (1985) A multiple-unit large-volume insitu filtration system for

sampling oceanic particulate matter in mesoscale environments. *Adv. Chem. Ser.*, 155–175.

Borrok D. M., Wanty R. B., Ridley W. I., Wolf R., Lamothe P. J. and Adams M. (2007) Separation of copper, iron, and zinc from complex aqueous solutions for isotopic measurement. *Chem. Geol.* **242**, 400–414.

Brantley S. L., Liermann L. and Bullen T. D. (2001) Fractionation of Fe isotopes by soil microbes and organic acids. *Geology* **29**, 535–538.

Bruland K. W. and Lohan M. C. (2003) Controls of trace metals in seawater. In (eds. H. D. Holland and K. H. Turekian). Elsevier.

Chapman J. B., Weiss D. J., Shan Y. and Lemburger M. (2009) Iron isotope fractionation during leaching of granite and basalt by hydrochloric and oxalic acids. *Geochim. Cosmochim. Acta* **73**, 1312–1324.

Chen H., Laskin A., Baltrusaitis J., Gorski C. A., Scherer M. M. and Grassian V. H. (2012) Coal fly ash as a source of iron in atmospheric dust. *Environ. Sci. Technol.* **46**, 2112–2120.

Chester R. and Hughes M. J. (1967) A chemical technique for the separation of ferromanganese minerals, carbonate minerals, and absorbed trace elements from pelagic sediment. *Chem. Geol.* **2**, 249–262.

Collier R. and Edmond J. (1984) The trace-element geochemistry of marine biogenic particulate matter. *Prog. Oceanogr.* **13**, 113–199.

Conway T. M., Rosenberg A. D., Adkins J. F. and John S. G. (2013) A new method for precise determination of iron, zinc and cadmium stable isotope ratios in seawater by double-spike mass spectrometry. *Anal. Chim. Acta* **793**, 44–52.

Cwiertny D. M., Baltrusaitis J., Hunter G. J., Laskin A., Scherer M. M. and Grassian V. H. (2008) Characterization and acid-mobilization study of iron-containing mineral dust source materials. *J. Geophys. Res.* **113**.

Dideriksen K., Baker J. A. and Stipp S. L. S. (2008) Equilibrium Fe isotope fractionation between inorganic aqueous Fe(III) and the siderophore complex, Fe(III)-desferrioxamine B. *Earth Planet. Sci. Lett.* **269**, 280–290.

Epstein E. (1971) *Mineral nutrition of plants: Principles and perspectives*. John Wiley and Sons.

Escoube R., Rouxel O. J., Sholkovitz E. and Donard O. F. X. X. (2009) Iron isotope systematics in estuaries: the case of North River, Massachusetts (USA). *Geochim. Cosmochim. Acta* **73**, 4045–4059.

Fehr M. A., Andersson P. S., Halenius U. and Morth C. M. (2008) Iron isotope variations in Holocene sediments of the Gotland Deep, Baltic Sea. *Geochim. Cosmochim. Acta* **72**, 807–826.

Gelting J., Breitbarth E., Stolpe B., Hassellöv M. and Ingri J. (2010) Fractionation of iron species and iron isotopes in the Baltic Sea euphotic zone. *Biogeosciences* **7**, 2489–2508.

Guelke M. and Von Blanckenburg F. (2007) Fractionation of stable iron isotopes in higher plants. *Environ. Sci. Technol.* **41**, 1896–1901.

Guelke M., von Blanckenburg F., Schoenberg R., Staubwasser M. and Stuetzel H. (2010) Determining the stable Fe isotope signature of plant-available iron in soils. *Chem. Geol.* **277**, 269–280.

Guelke-Stelling M. and von Blanckenburg F. (2012) Fe isotope fractionation caused by translocation of iron during growth of bean and oat as models of strategy I and II plants. *Plant Soil* **352**, 217–231.

Hawkings J. R., Wadham J. L., Tranter M., Raiswell R., Benning L. G., Statham P. J., Tedstone A., Nienow P., Lee K. and Telling J. (2014) Ice sheets as a significant source of highly reactive nanoparticulate iron to the oceans. *Nat. Commun.* **5**.

Jickells T. D., An Z. S., Andersen K. K., Baker A. R., Bergametti G., Brooks N., Cao J. J., Boyd P. W., Duce R. A., Hunter K. A., Kawahata H., Kubilay N., laRoche J., Liss P. S., Mahowald N., Prospero J. M., Ridgwell A. J., Tegen I. and Torres R. (2005) Global iron connections between desert dust, ocean biogeochemistry, and climate. *Science* **308**, 67–71.

John S. G. (2012) Optimizing sample and spike concentrations for isotopic analysis by double-spike ICPMS. *J. Anal. At. Spectrom.* **27**, 2123.

Johnson C. M., Skulan J. L., Beard B. L., Sun H., Nealson K. H. and Braterman P. S. (2002) Isotopic fractionation between Fe(III) and Fe(II) in aqueous solutions. *Earth Planet. Sci. Lett.* **195**, 141–153.

Kiczka M., Wiederhold J. G., Frommer J., Kraemer S. M., Bourdon B. and Kretzschmar R. (2010a) Iron isotope fractionation during proton- and ligand-promoted dissolution of primary phyllosilicates. *Geochim. Cosmochim. Acta* **74**, 3112–3128.

Kiczka M., Wiederhold J. G., Kraemer S. M., Bourdon B. and Kretzschmar R. (2010b) Iron isotope fractionation during Fe uptake and translocation in Alpine plants. *Environ. Sci. Technol.* **44**, 6144–6150.

Lam P. J. and Bishop J. K. B. (2008) The continental margin is a key source of iron to the HNLC North Pacific Ocean. *Geophys. Res. Lett.* **35**, L07608.

Lam P. J., Bishop J. K. B., Henning C. C., Marcus M. A., Waychunas G. A. and Fung I. Y. (2006) Wintertime phytoplankton bloom in the subarctic Pacific supported by continental margin iron. *Global Biogeochem. Cycles* **20**.

Lovely D. ed. (2000) Environmental Microbe-Metal Interactions.

Martinez N., Murray R., Thunell R., Peterson L., Mullerkarger F., Astor Y. and Varela R. (2007) Modern climate forcing of terrigenous deposition in the tropics (Cariaco Basin, Venezuela). *Earth Planet. Sci. Lett.* **264**, 438–451.

Moore J. K. and Braucher O. (2008) Sedimentary and mineral dust sources of dissolved iron to the world ocean. *Biogeosciences* **5**, 631–656.

Moore C. M., Mills M. M., Arrigo K. R., Berman-Frank I., Bopp L., Boyd P. W., Galbraith E. D., Geider R. J., Guieu C., Jaccard S. L., Jickells T. D., La Roche J., Lenton T. M., Mahowald N. M., Maranon E., Marinov I., Moore J. K., Nakatsuka T., Oschlies A., Saito M. A., Thingstad T. F., Tsuda A. and Ulloa O. (2013) Processes and patterns of oceanic nutrient limitation. *Nat. Geosci.* **6**, 701–710.

Naidu A. S., Burrell D. C. and Hood D. W. (1971) Clay mineral composition and geologic significance of some Beaufort Sea sediments. *J. Sediment. Petrol.* **41**, 691.

Poulton S. W. and Canfield D. E. (2005) Development of a sequential extraction procedure for iron: implications for iron partitioning in continentally derived particulates. *Chem. Geol.* **214**, 209–221.

Radic A., Lacan F. and Murray J. W. (2011) Iron isotopes in the seawater of the equatorial Pacific Ocean: new constraints for the oceanic iron cycle. *Earth Planet. Sci. Lett.* **306**, 1–10.

Raiswell R., Tranter M., Benning L. G., Siegert M., De'ath R., Huybrechts P. and Payne T. (2006) Contributions from glacially derived sediment to the global iron (oxyhydr)oxide cycle: implications for iron delivery to the oceans. *Geochim. Cosmochim. Acta* **70**, 2765–2780.

Rauschenberg S. and Twining B. S. (2015) Evaluation of approaches to estimate biogenic particulate trace metals in the ocean. *Mar. Chem.* **171**, 67–77.

Revels B. N., Ohnemus D. C., Lam P. J., Conway T. M. and John S. G. (2014) The isotope signature and distribution of particulate iron in the North Atlantic ocean. *Deep Sea Res. Part II.*

Roy M., Rouxel O., Martin J. B. and Cable J. E. (2012) Iron isotope fractionation in a sulfide-bearing subterranean estuary

and its potential influence on oceanic Fe isotope flux. *Chem. Geol.* **300–301**, 133–142.

Rue E. L. and Bruland K. W. (1995) Complexation of iron(III) by natural organic ligands in the Central North Pacific as determined by a new competitive ligand equilibration adsorptive cathodic stripping voltammetric method. *Mar. Chem.* **50**, 117–138.

Severmann S., Johnson C. M., Beard B. L., German C. R., Edmonds H. N., Chiba H. and Green D. R. H. (2004) The effect of plume processes on the Fe isotope composition of hydrothermally derived Fe in the deep ocean as inferred from the Rainbow vent site, Mid-Atlantic Ridge, 36°14′N. *Earth Planet. Sci. Lett.* **225**, 63–76.

Severmann S., Johnson C. M., Beard B. L. and McManus J. (2006) The effect of early diagenesis on the Fe isotope compositions of porewaters and authigenic minerals in continental margin sediments. *Geochim. Cosmochim. Acta* **70**, 2006–2022.

Sherrell R. M. and Boyle E. A. (1992) The trace-metal composition of suspended particles in the oceanic water column near Bermuda. *Earth Planet. Sci. Lett.* **111**, 155–174.

Staubwasser M., von Blanckenburg F. and Schoenberg R. (2006) Iron isotopes in the early marine diagenetic iron cycle. *Geology* **34**, 629–632.

Staubwasser M., Schoenberg R., von Blanckenburg F., Krüger S. and Pohl C. (2013) Isotope fractionation between dissolved and suspended particulate Fe in the oxic and anoxic water column of the Baltic Sea. *Biogeosciences* **10**, 233–245.

Tang D. G. and Morel F. M. M. (2006) Distinguishing between cellular and Fe-oxide-associated trace elements in phytoplankton. *Mar. Chem.* **98**, 18–30.

Tessier A., Campbell P. G. C. and Bisson M. (1979) Sequential extraction procedure for the speciation of particulate trace metals. *Anal. Chem.* **51**, 844–851.

Tovar-Sanchez A., Sañudo-Wilhelmy S., Garcia-Vargas M., Weaver R. S., Popels L. C., Hutchins D. A. and Sanudo-Wilhelmy S. A. (2003) A trace metal clean reagent to remove surface-bound iron from marine phytoplankton. *Mar. Chem.* **82**, 91–99.

Viollier E., Inglett P., Hunter K. A., Roychoudhury A. and Van Cappellen P. (2000) The ferrozine method revisited: Fe(II)/Fe(III) determination in natural waters. *Appl. Geochem.* **15**, 785–790.

Waeles M., Baker A. R., Jickells T. and Hoogewerff J. (2007) Global dust teleconnections: aerosol iron solubility and stable isotope composition. *Environ. Chem.* **4**, 233–237.

Wiederhold J. G., Kraemer S. M., Teutsch N., Borer P. M., Halliday A. N. and Kretzschmar R. (2006) Iron isotope fractionation during proton-promoted, ligand-controlled, and reductive dissolution of goethite. *Environ. Sci. Technol.* **40**, 3787–3793.

Wiederhold J. G., Teutsch N., Kraemer S. M., Halliday A. N. and Kretzschmar R. (2007) Iron isotope fractionation in oxic soils by mineral weathering and podzolization. *Geochim. Cosmochim. Acta* **71**, 5821–5833.

Wu J. F. and Luther G. W. (1995) Complexation of Fe(III) by natural organic ligands in the Northwest Atlantic Ocean by a competitive ligand equilibration method and a kinetic approach. *Mar. Chem.* **50**, 159–177.

Associate editor: Andrew Ross Bowie